Springer

KSME

Journal of Mechanical Science and Technology 24 (10) (2010) 2107~2117
www.springerlink.com/content/1738-494x
DOI 10.1007/s12206-010-0701-0

Semi-analytical solution of magneto-thermo-elastic stresses for functionally graded variable thickness rotating disks †

A. Ghorbanpour Arani*, A. Loghman, A. R. Shajari and S. Amir

Department of Mechanical Engineering, Faculty of Engineering, University of Kashan, Kashan, I.R. Iran

(Manuscript Received April 16, 2010; Revised June 24, 2010; Accepted June 30, 2010)

Abstract

In this paper, a semi-analytical solution for magneto-thermo-elastic problem in functionally graded (FG) hollow rotating disks with variable thickness placed in uniform magnetic and thermal fields is presented. Stresses and perturbation of magnetic field vector in FG rotating disks are determined using infinitesimal theory of magneto-thermo-elasticity under plane stress conditions. The material properties except Poisson's ratio are modeled as power-law distribution of volume fraction. The profile of disk thickness is assumed to be a parabolic function of radius. The non-dimensional distribution of temperature, displacement, stresses and perturbation of magnetic field vector throughout radius are shown. Effects of material grading index, geometry of the disk and magnetic field on the stress and displacement fields are investigated. The results of stresses and radial displacements for two different boundary conditions with and without the effect of magnetic field are compared for a FG rotating disk with concave thickness profile. It has been found that imposing a magnetic field significantly decreases tensile circumferential stresses. Therefore the fatigue life of the disk will be significantly improved by applying the magnetic field. Results of this investigation could be applied for optimum design of FG hollow rotating disks with variable thickness.

Keywords: FGM; Magneto-thermo-elastic; Hollow rotating disk; Perturbation of magnetic field vector; Plane stress; Variable thickness

1. Introduction

The functionally graded materials (FGMs) have attracted much attention in recent years. In such materials, the properties are varied continuously according to a position function, along certain direction of the structure. Indeed, FGMs are combinations of two material phases that has been intentionally graded from one material at one surface to another material at the opposite one.

The first idea for producing FGMs was their application in high temperature environment and improving their mechanical properties. These materials which are mainly constructed to operate in high temperature environments, find their application in nuclear reactors, chemical laboratories, aerospace, turbine rotors, flywheels and pressure vessels. As the use of FGMs increases, new methodologies need to be developed to characterize, analyze and design structural components made of these materials. There are some studies dealing with elastic and thermo-elastic problems of FGMs components but few studies can be found on the magneto-thermo-elastic behavior of such components in the literature.

Suresh and Mortensen [1] have provided an introduction to the fundamentals of FGMs. Lutz and Zimmerman [2, 3] obtained analytical solutions for the stresses in spheres and cylinders made of FGMs. They considered thick spheres and cylinders under radial thermal loads with a linear composition of the constituent materials. Hosseini Kordkheili and Naghdabadi [4] investigated the relative influences of basic factors such as property gradation index and loading conditions on stresses and deformations of a FG rotating disk. Obata and Noda [5] studied the thermal stresses in a FG circular hollow cylinder and a hollow sphere using the perturbation method assuming one-dimensional steady-state conditions.

Dai and Fu [6] considered the magneto-thermo-elastic problem of FGM hollow structures subjected to mechanical loads. They assumed that the material properties to be a simple power-law variation through the structure's wall thickness. Using the infinitesimal theory of elasticity, Dai et al. [7] analyzed the magneto-thermo-elastic behavior of FGM cylindrical and spherical vessels subjected to an internal pressure and a uniform magnetic field.

Ghorbanpour et al. [8] presented an analytical method to obtain the transient response of magneto-thermo-elastic stress and perturbation of the magnetic field vector for a thick-

† This paper was recommended for publication in revised form by Associate Editor Seong Beom Lee

* Corresponding author. Tel.: +98 9131626594, Fax: +98 361 5559930
E-mail address: aghorban@kashanu.ac.ir; a_ghorbanpour@yahoo.com.

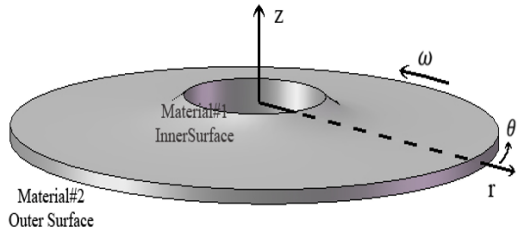

Fig. 1. Configuration of a thin FG rotating disk with variable thickness.

walled spherical vessel made of FGMs. They studied the effect of magnetic field vector and material in-homogeneity on the stresses in FGM hollow sphere. They concluded that their analyses and numerical results presented are accurate and reliable and may be used as a reference to solve other dynamic coupled problems in an FGM hollow sphere placed in a uniform magnetic field, subjected to mechanical load and thermal shock.

Ghorbanpour et al. [9] presented a closed-form solution for one-dimensional magneto-thermo-elastic problem in a FGM hollow sphere placed in uniform magnetic and distributed temperature fields subjected to an internal pressure using the infinitesimal theory of magneto-thermo-elasticity. Their results are applicable for optimum design of FGM hollow spheres.

Tang [10] presented an elastic solution for anisotropic rotating disks. Ruhi et al. [11] presented a semi-analytical solution for thick-walled finitely-long cylinders made of FGMs under thermo mechanical load. Reddy et al. [12] analyzed elastic stresses in a rotating anisotropic annular disk of variable thickness and variable density. Eraslan et al. [13] investigated the elastic-plastic behavior of rotating variable thickness annular disks with free, pressurized and radially constrained boundary conditions. Guven [14] presented the analysis of elastic-plastic stress in a rotating annular disk with variable thickness and variable density.

In this paper, the FG rotating disks with variable thickness are considered (Fig. 1). The material's thermal, mechanical and magnetic properties are assumed to be the same power-law distribution of volume fraction content. The thickness profile of the FG disk is assumed to be parabolic function of the radius. Plane stress and axisymmetry conditions are assumed.

The main objective of this study is to investigate the effect of magnetic and temperature fields on stresses and deformations of FG hollow rotating disks. The effect of boundary conditions and material properties are also investigated. A semi-analytical method is employed to obtain the magneto-thermo-elastic solution for the temperature, displacement, stresses and perturbation of magnetic field vector in the FG disks. In this method, the radial domain is divided into a large number of sub domains in which the radial dependent thermal, mechanical and magnetic properties are considered to have constant values at thin layer of each sub domain. Therefore the governing differential equations of the disk can be solved for a thin layer with constant coefficients. Satisfying the conditions of continuity at the inner and outer surfaces of each sub domain and finally satisfying the global boundary conditions magneto-thermo-elastic stresses, displacements and perturbation of magnetic field vector are reported in this work. Increasing the number of divisions in the radial direction increases the accuracy of the results.

2. Property Gradation

In this study all mechanical, thermal and magnetic properties except Poisson's ratio are assumed to be in the following form:

$$P(r) = (P_o - P_i)\left(\frac{r - r_i}{r_o - r_i}\right)^n + P_i;\ r_i < r < r_o, \tag{1}$$

where P_i, P_o are the properties at the inner and outer surfaces of the disk; r_i and r_o are the inner and outer radii of the disk, respectively. Here the function $P(r)$ is abbreviated with P_r. In this study $n \geq 0$ (grading index) is the volume fraction exponent that indicates the material variation profile along the radius.

The non-dimensional solution is presented in this study in which the non-dimensional variables are defined as follows:

$$\begin{aligned} &R = \frac{r}{r_o};\quad R_i = \frac{r_i}{r_o};\quad R_i < R < 1, \\ &\overline{P_R} = \overline{P(R)} = (1 - \overline{P_{R_i}})\left(\frac{R - R_i}{1 - R_i}\right)^n + \overline{P_{R_i}};\quad \overline{P_{R_i}} = \frac{P(r_i)}{P(r_o)}. \end{aligned} \tag{2}$$

3. Definition of disk thickness profile

The thickness profile of the disk is assumed to be a parabolic function of radius according to the following form:

$$z(r) = z_a\left(1 - q\left(\frac{r}{r_o}\right)^m\right), \tag{3}$$

where z_a is virtual thickness at central axis, q and m are geometric parameters that determine concavity of the disk thickness profile as follows:

$$\begin{aligned} &q \neq 0,\ m < 1 \Rightarrow \text{Concave}, \\ &q \neq 0,\ m = 1 \Rightarrow \text{Linear}, \\ &q \neq 0,\ m > 1 \Rightarrow \text{Convex}, \\ &q = 0 \Rightarrow \text{Constant thickness}. \end{aligned} \tag{4}$$

In this study the non-dimensional form for thickness profile has been used

$$\begin{aligned} &Z_R = 1 - qR^m, \\ &Z_R = \frac{z(r)}{z_a}, \end{aligned} \tag{5}$$

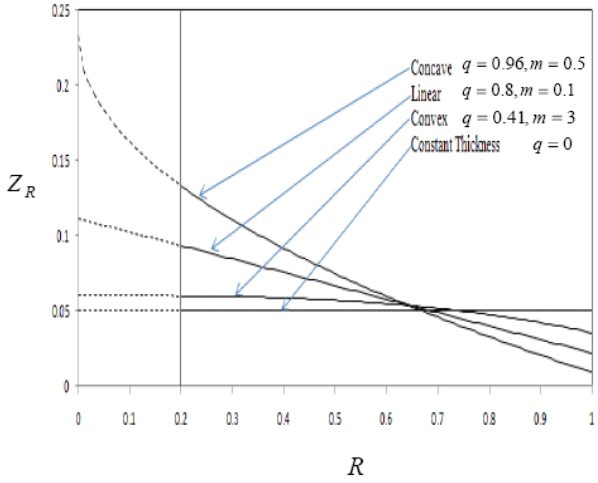

Fig. 2. Variation of non-dimensional thickness profiles of FG disk versus non-dimensional radius for different values of q and m.

where Z_R is non-dimensional thickness profile of the disk and R is non-dimensional radius as defined in Eq. (2). The variation of non-dimensional thickness profiles $Z_R = z(r)/z_a$ with non-dimensional radius $R = r/r_o$ for different values of q and m are shown in Fig. 2.

4. Boundary conditions

The following traction conditions on the inner and outer surfaces of the rotating hollow disk must be satisfied.

4.1 Hollow disk with free-free boundary condition

$$\begin{aligned} &\sigma_r = 0; \quad r = r_i, \\ &\sigma_r = 0; \quad r = r_o. \end{aligned} \tag{6}$$

4.2 Hollow disk with fixed-free boundary condition

$$\begin{aligned} &u = 0; \quad r = r_i, \\ &\sigma_r = 0; \quad r = r_o. \end{aligned} \tag{7}$$

The non-dimensional forms of the above boundary conditions are as following:

(a) Free-free boundary conditions

$$\begin{aligned} &\overline{\sigma_R} = 0; \quad R = R_i, \\ &\overline{\sigma_R} = 0; \quad R = 1. \end{aligned} \tag{8}$$

(b) Fixed-free boundary conditions

$$\begin{aligned} &U = 0; \quad R = R_i, \\ &\overline{\sigma_R} = 0; \quad R = 1. \end{aligned} \tag{9}$$

5. Heat conduction problem

The first law of thermodynamics for energy equation in the steady-state conduction without energy generation for an axisymmetric FG one-dimensional disk is given by

$$\frac{1}{r}\frac{\partial}{\partial r}[rz(r)k(r)\frac{\partial T}{\partial r}] = 0. \tag{10}$$

It is assumed that the non-homogeneous thermal conductivity $k_r = k(r)$ is also a power-law function of volume fraction

$$k(r) = (k_o - k_i)(\frac{r - r_i}{R_o - r_i})^n + k_i. \tag{11}$$

The non-dimensional temperature gradient is defined as

$$\overline{\Delta T_R} = \frac{T - T_i}{T_o - T_i}, \tag{12}$$

where T_i and T_o are temperatures at the inner and the outer surfaces of FG disk, respectively.

Substituting non-dimensional variables of Eqs. (2), (5) and (12) into heat conduction equation Eq. (10) yields

$$\frac{d^2\overline{\Delta T_R}}{dR^2} + (\frac{1}{R} + \frac{1}{\overline{K}(R)}\frac{d\overline{K}(R)}{dR} + \frac{1}{Z(R)}\frac{dZ(R)}{dR})\frac{d\overline{\Delta T_R}}{dR} = 0, \tag{13}$$

where $\overline{K_R}$ is non-dimensional thermal conductivity, which is defined according to Eq. (2).

Eq. (13) is a second order ordinary differential equation (ODE) with variable coefficients. Due to complication of coefficients, semi-analytical method for solution has been used. For this purpose, the solution domain is divided into several divisions (as shown in Fig. 3) and the coefficients of Eq. (13) are evaluated at $R^{(k)}$, mean radius of kth division and the ODE with constant coefficients valid only in kth subdomain turns out to be

$$(\frac{d^2}{dR^2} + \bar{c}^{(k)}\frac{d}{dR})\overline{\Delta T_{R^{(k)}}} = 0, \tag{14}$$

where

$$\bar{c}^{(k)} = \frac{1}{R^{(k)}} + \frac{1}{\overline{K_{R^{(k)}}}}\frac{d\overline{K_R}}{dR}\bigg|_{R=R^{(k)}} + \frac{1}{Z_{R^{(k)}}}\frac{dZ_R}{dR}\bigg|_{R=R^{(k)}}; \quad k = 1,2,...,m. \tag{15}$$

Now the 2nd order ODE with variable coefficients is converted into 2nd order ODE with constant coefficients for each division.

The exact solution for these types of ODEs can be written as

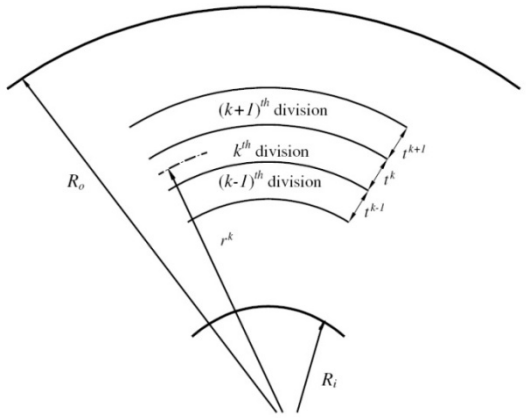

Fig. 3. Dividing radial domain into some finite sub-domains.

$$\overline{\Delta T_{R(k)}} = \overline{X}_1^{(k)} + \overline{X}_2^{(k)} \exp(-\overline{R^{(k)}}\overline{c}^{(k)}), \tag{16}$$

where $\overline{X}_1^{(k)}$ and $\overline{X}_2^{(k)}$ are unknowns constants for kth division. These unknowns are determined by applying the necessary boundary conditions between each two adjacent sub-domains.

The continuity of the value of temperature and the continuity of the heat flux are imposed at the interfaces of the adjacent sub-domains. These continuity conditions at the interfaces are

$$\begin{aligned} &\overline{\Delta T_R}\Big|_{R=R^k+\frac{t^k}{2}} = \overline{\Delta T_R}\Big|_{R=R^{k+1}-\frac{t^{k+1}}{2}}, \\ &\frac{d\overline{\Delta T_R}}{dR}\Big|_{R=R^k+\frac{t^k}{2}} = \frac{d\overline{\Delta T_R}}{dR}\Big|_{R=R^{k+1}-\frac{t^{k+1}}{2}}, \end{aligned} \tag{17}$$

The surface temperature imposed on inner and outer surfaces of FG hollow disk are

$$\begin{aligned} &\overline{\Delta T_R} = \overline{\Delta T_i} = 0 \quad \text{at} \quad R = R_i, \\ &\overline{\Delta T_R} = \overline{\Delta T_o} = 1 \quad \text{at} \quad R = R_o = 1. \end{aligned} \tag{18}$$

The continuity conditions Eq. (17) together with the global boundary conditions Eq. (18) yield a set of linear algebraic equations in terms of $\overline{X}_1^{(k)}$ and $\overline{X}_2^{(k)}$. Solving these equations for $\overline{X}_1^{(k)}$ and $\overline{X}_2^{(k)}$. Then, temperature $\overline{\Delta T_R}$ is determined in each radial sub-domain.

6. Magneto-thermo-elastic solution

The disk is placed in a uniform magnetic field $\vec{H}(0,0,H_z)$ and rotating with constant angular velocity ω. The rotation creates a centrifugal force that is used as a radial dependent body force in equilibrium equation.

Since the disck is thin, the plane stress condition is considered. Moreover, cylindrical coordinate system is used and axial symmetry is assumed.

For the axisymmetric plane stress problem, the constitutive relations are

$$\varepsilon_{rr} = \frac{du}{dr}, \ \varepsilon_{\theta\theta} = \frac{u}{r}, \tag{19}$$

$$\sigma_r = \frac{E}{1-\nu^2}\left(\varepsilon_r + \nu\varepsilon_\theta - (1+\nu)\alpha_r \Delta T(r)\right), \tag{20}$$

$$\sigma_\theta = \frac{E}{1-\nu^2}\left(\varepsilon_\theta + \nu\varepsilon_r - (1+\nu)\alpha_r \Delta T(r)\right), \tag{21}$$

where α_r is the thermal expansion coefficient.

Assuming that magnetic permeability $\mu(r)$ is a power-law function of volume fraction according to Eq. (2). The governing electro-dynamic Maxwell equations [15] for a perfectly conducting elastic body can be written as

$$\begin{aligned} &\vec{J} = \nabla \times \vec{h}, \quad \nabla \times \vec{e} = -\mu(r)\frac{\partial \vec{h}}{\partial t}, \quad div\, \vec{h} = 0, \\ &\vec{e} = -\mu(r)(\frac{\partial \vec{U}}{\partial t} \times \vec{H}), \quad \vec{h} = \nabla \times (\vec{U} \times \vec{H}). \end{aligned} \tag{22}$$

Applying an initial magnetic field vector $\vec{H}(0,0,H_z)$ in the cylindrical coordinates to Eq. (22), yields

$$\begin{aligned} &\vec{U} = (u,0,0), \quad \vec{e} = -\mu(r)(0, H_z\frac{\partial u}{\partial t}, 0), \\ &\vec{h} = (0,0,h_z), \quad \vec{J} = (0, -\frac{\partial h_z}{\partial t}, 0), \\ &h_z = -H_z(\frac{\partial u}{\partial r} + \frac{u}{r}). \end{aligned} \tag{23}$$

The equilibrium equation of the FG hollow rotating disk under centrifugal body force is expressed as

$$\frac{\partial(z(r)\sigma_r)}{\partial r} + z(r)\frac{\sigma_r - \sigma_\theta}{r} + z(r)f_z + \rho(r)z(r)r\omega^2 = 0, \tag{24}$$

where f_z is the Lorentz's force [9, 15] as following

$$f_z = \mu(r)(\vec{J} \times \vec{H}) = \mu(r)H_z^2\frac{\partial}{\partial r}(\frac{\partial u}{\partial r} + \frac{u}{r}). \tag{25}$$

To obtain the equilibrium equation in terms of the displacement for the FG rotating disk, the functional relationships of the material properties have to be known. The variation of property along the radius, as explained in sec. (2) is a power-law distribution of volume fraction

$$
\begin{aligned}
E_r &= E(r) = (E_o - E_i)(\frac{r-r_i}{r_o-r_i})^n + E_i,\\
\alpha_r &= \alpha(r) = (\alpha_o - \alpha_i)(\frac{r-r_i}{r_o-r_i})^n + \alpha_i,\\
\rho_r &= \rho(r) = (\rho_o - \rho_i)(\frac{r-r_i}{r_o-r_i})^n + \rho_i,\\
\mu_r &= \mu(r) = (\mu_o - \mu_i)(\frac{r-r_i}{r_o-r_i})^n + \mu_i,
\end{aligned}
\tag{26}
$$

and thickness profile of the disk can be obtained from Eq. (3).

Substituting property distribution Eq. (26) and stress relation Eqs. (20) and (21) into Eq. (24) yields an ODE in terms of radial displacement which is navier's equation:

$$
C_1\frac{d^2u}{dr^2} + C_2\frac{du}{dr} + C_3u + C_4 = 0, \tag{27}
$$

where

$$
\begin{aligned}
C_1 &= rz(r)\Big(E(r) + \mu(r)H_z{}^2(1-\nu^2)\Big),\\
C_2 &= z(r)\mu(r)H_z{}^2(1-\nu^2) + \frac{d}{dr}\big(rz(r)E(r)\big),\\
C_3 &= -\frac{1}{r}z(r)\Big(E(r) + \mu(r)H_z{}^2(1-\nu^2)\Big)\\
&\quad + \nu\frac{d}{dr}\big(z(r)E(r)\big),\\
C_4 &= z(r)\rho(r)r^2\omega^2(1-\nu^2)\\
&\quad - r\frac{d}{dr}\big(z(r)E(r)(1+\nu)\alpha(r)\Delta T(r)\big).
\end{aligned}
\tag{28}
$$

It is shown that non-homogenous term (C_4) of Eq. (27) is resulting of rotating and thermal field. According to the non-dimensional form Eqs. (2), (5) and (12), these relations can be written as

$$
\left(\overline{C_1}\frac{d^2}{dR^2} + \overline{C_2}\frac{d}{dR} + \overline{C_3}\right)U + \overline{C_4} = 0, \tag{29}
$$

where

$$
\begin{aligned}
\overline{C_1} &= z_aRZ_R\Big(E_o\,\overline{E_R} + \mu_o\,\overline{\mu_R}H_z{}^2(1-\nu^2)\Big),\\
\overline{C_2} &= \mu_o z_a Z_R\,\overline{\mu_R}H_z{}^2(1-\nu^2) + z_aE_o\frac{d\left(RZ_R\overline{E_R}\right)}{dR},\\
\overline{C_3} &= -\frac{1}{R}z_aZ_R\Big(E_o\,\overline{E_R} + \mu_o\,\overline{\mu_R}H_z{}^2(1-\nu^2)\Big)\\
&\quad + \nu z_aE_o\frac{d(Z_R\overline{E_R})}{dR},\\
\overline{C_4} &= \frac{\rho_o r_o^3\omega^2 z_a}{u_o}(1-\nu^2)\overline{\rho_R}Z_RR^2\\
&\quad - \frac{r_o\Delta T_o\alpha_o z_aE_o(1+\nu)}{u_o}R\frac{d\left(\overline{E_R}Z_R\overline{\alpha_R\Delta T_R}\right)}{dR},
\end{aligned}
\tag{30}
$$

and

$$
\begin{aligned}
U &= \frac{u}{u_o},\\
u_o &= \rho_o r_o{}^3\omega^2 + (1+\nu)E_or_o\alpha_o\Delta T_o.
\end{aligned}
\tag{31}
$$

Eq. (29) is non-homogenous 2nd order ODE with variable coefficients. Similar to solution of heat conduction equation, the semi-analytical method must be employed.

The navier's equation yields

$$
\left(C_1^{(k)}\frac{d^2}{dR^2} + C_2^{(k)}\frac{d}{dR} + C_3^{(k)}\right)U^{(k)} + C_4^{(k)} = 0. \tag{32}
$$

The coefficients of Eq. (32) are evaluated in each division in terms of constants and the radius of *k*th division.

$$
\begin{aligned}
C_1^{(k)} &= z_aR^{(k)}Z_{R^{(k)}}\left(E_o\,\overline{E_{R^{(k)}}} + \mu_o\,\overline{\mu_{R^{(k)}}}H_z{}^2(1-\nu^2)\right),\\
C_2^{(k)} &= \mu_o z_a Z_{R^{(k)}}\,\overline{\mu_{R^{(k)}}}H_z{}^2(1-\nu^2)\\
&\quad + z_aE_o\frac{d}{dR}\Big|\left(RZ_R\overline{E_R}\right)_{R=R^{(k)}},\\
C_3^{(k)} &= -\frac{1}{R^{(k)}}z_aZ_{R^{(k)}}(\mu_o\,\overline{\mu_{R^{(k)}}}H_z{}^2(1-\nu^2)\\
&\quad + E_o\,\overline{E_{R^{(k)}}}) + \nu z_aE_o\frac{d(Z_R\overline{E_R})}{dR}\Big|_{R=R^{(k)}},\\
C_4^{(k)} &= \frac{\rho_o r_o^3\omega^2 z_a}{u_o}(1-\nu^2)\overline{\rho_{R^{(k)}}}Z_{R^{(k)}}\left(R^{(k)}\right)^2\\
&\quad - \frac{r_o\Delta T_o\alpha_o z_aE_o(1+\nu)}{u_o}R^{(k)}\frac{d}{dR}\left(\overline{E_R}Z_R\overline{\alpha_R\Delta T_R}\right)\Big|_{R=R^{(k)}}.
\end{aligned}
\tag{33}
$$

The exact general solution for Eq. (32) can be written in the form of

$$
U^{(k)} = X_1^{(k)}\exp(\eta_1{}^{(k)}R) + X_2{}^{(k)}\exp(\eta_2{}^{(k)}R) - \frac{C_4^{(k)}}{C_3^{(k)}}, \tag{34}
$$

where

$$
\eta_1{}^{(k)},\eta_2{}^{(k)} = \frac{C_2{}^{(k)} \pm \sqrt{(C_2{}^{(k)})^2 - 4C_3{}^{(k)}C_1{}^{(k)}}}{2C_1{}^{(k)}}. \tag{35}
$$

It is noted that this solution for Eq. (32) is valid in

$$
R^{(k)} - \frac{t^{(k)}}{2} \le R \le R^{(k)} + \frac{t^{(k)}}{2}. \tag{36}
$$

In Eq. (34) $X_1^{(k)}$ and $X_2{}^{(k)}$ are unknown constants for *k*th division which are determined by applying the necessary boundary conditions between two adjacent sub-domains. For this purpose, the continuity of the radial displacement U as

well as radial stress $\overline{\sigma_R}$ is imposed at the interfaces of the adjacent sub-domains. These continuity conditions at the interfaces are

$$\begin{aligned} &U^{(k)}\Big|_{R=R^{(k)}+\frac{t^{(k)}}{2}} = U^{(k)}\Big|_{R=R^{(k+1)}-\frac{t^{(k+1)}}{2}}, \\ &\overline{\sigma_R{}^{(k)}}\Big|_{R=R^{(k)}+\frac{t^{(k)}}{2}} = \overline{\sigma_R{}^{(k)}}\Big|_{R=R^{(k+1)}-\frac{t^{(k+1)}}{2}}. \end{aligned} \tag{37}$$

The continuity conditions Eq. (37) together with the global boundary conditions Eqs. (8) and (9) yield a set of linear algebraic equations in terms of $X_1^{(k)}$ and $X_2^{(k)}$. Solving the resultant linear algebraic equations for $X_1^{(k)}$ and $X_2^{(k)}$, the unknown coefficients of Eq. (34) are calculated. Then, the non-dimensional displacement component U is determined in each radial sub-domain. Increasing the number of subdivisions improves the accuracy of the results.

7. Numerical results and discussion

To illustrate the results of magneto-thermo-elastic solution in this study, a rotating FG disk with $R_0 = 5R_i$ is considered with non-dimensional form for material properties as explained in Sec. 2. Following Ghorbanpour et al. [9] the magnetic intensity is taken as $H_z = 2.23\times10^9\, A/m$.

The analysis for two cases of hollow disk with free-free boundary condition and hollow disk with fixed-free boundary conditions has been carried out. The results for temperature, radial displacement, magneto-thermo-elastic stresses and the perturbation of the magnetic field vector for the FG rotating disk are presented. The following material properties are used in computing the numerical results:

$$\begin{aligned} &E_i = 70\,Gpa, && E_o = 151\,Gpa, \\ &\rho_i = 2700\frac{kg}{m^3}, && \rho_o = 5700\frac{kg}{m^3}, \\ &\alpha_{r_i} = 23\times10^{-6}\frac{1}{{}^oC}, && \alpha_{r_o} = 10\times10^{-6}\frac{1}{{}^oC}, \\ &\mu_i = 1.256665081\times10^{-6}\frac{H}{m}, \\ &\mu_o = 2.63225901\times10^{-6}\frac{H}{m}, \\ &K_i = 209\frac{W}{m\,{}^oC}, && K_o = 20\frac{W}{m\,{}^oC}, \\ &\nu = 0.3, && \overline{\Delta T_i} = 0, \overline{\Delta T_o} = 1, && \omega = 1200\,rpm. \end{aligned} \tag{38}$$

The value of grading index n in this solution is taken 0, 0.2, 0.5, 1.5, 2, 5 and infinity. Obviously the zero value for n indicates full ceramic and infinity indicates full metal.

7.1 Magneto-thermo-elastic results

7.1.1 Free-free boundary condition

Fig. 4 illustrates the distribution of non-dimensional temperature versus dimensionless radius for various values of grading index n along the thickness of the FG disk. It shows that for homogenous cases whether metal or ceramic, the non-dimensional temperature distributions are the same. The steady-state temperature distribution in FG or homogeneous disk of concave profile is lower than convex, linear or constant profiles. The thermal boundary conditions are also satisfied.

Figs. 5 and 6 show the variation of non-dimensional radial

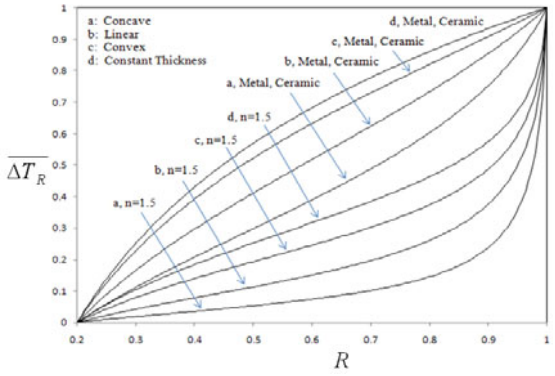

Fig. 4. Distribution of non-dimensional temperature change along the radius of FG disk for constant, linear, convex and concave thickness profiles.

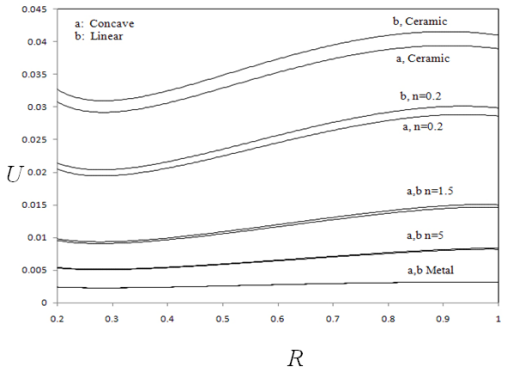

Fig. 5. Distribution of non-dimensional radial displacement for concave and linear thickness profiles.

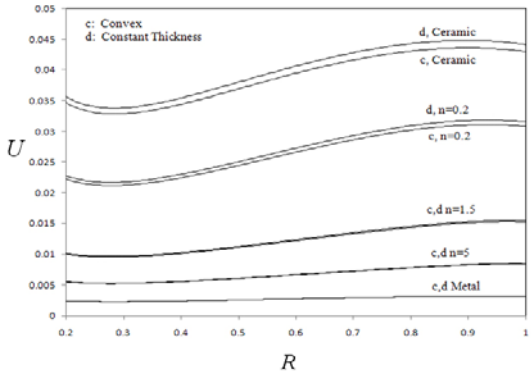

Fig. 6. Distribution of non-dimensional radial displacement for convex and constant thickness profiles.

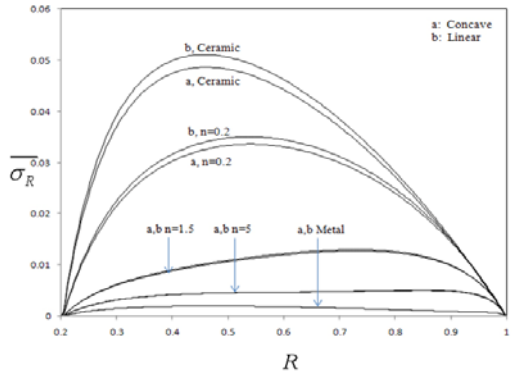

Fig. 7. Distribution of non-dimensional radial stress for concave and linear thickness profiles.

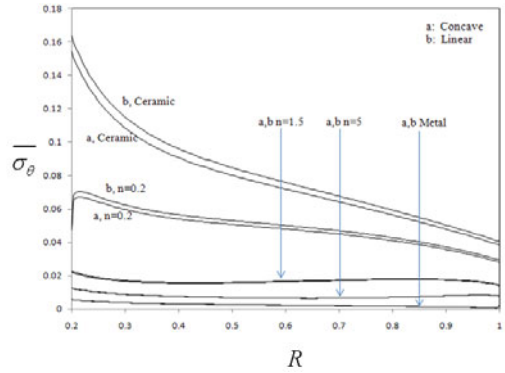

Fig. 9. Distribution of non-dimensional circumferential stress for concave and linear thickness profiles.

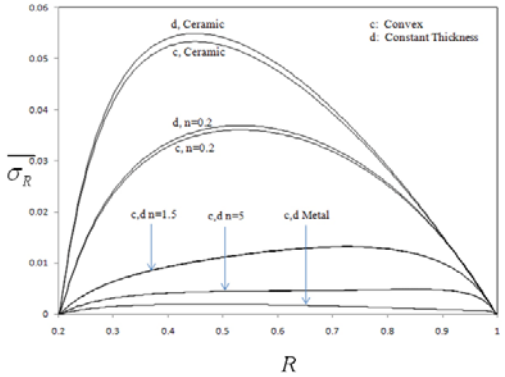

Fig. 8. Distribution of non-dimensional radial stress for convex and constant thickness profiles.

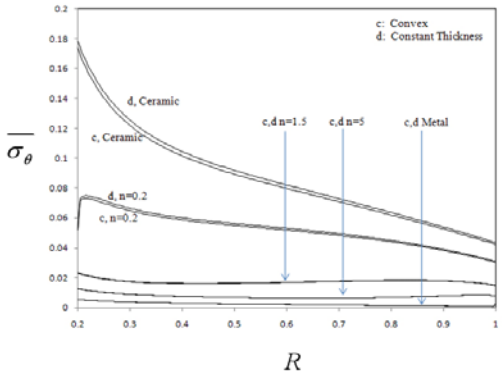

Fig. 10. Distribution of non-dimensional circumferential stress for convex and constant thickness profiles.

displacement versus radius for different values of grading index n and different thickness profiles. For different thickness profiles, it can be seen from Figs. 5 and 6 that the displacement increases when the grading index decreases, so the maximum and minimum displacements belong to pure ceramic and pure metal respectively. For all values of grading index n, the minimum displacement is located near the inner surface of the disk and its maximum is located near the outer surface of the disk.

Figs. 7, 8, 9 and 10 represent the variation of non-dimensional radial and circumferential stresses versus dimensionless radius respectively for different thickness profiles and material grading index. The mechanical free-free boundary conditions are well satisfied in Figs. 7 and 8. It is obvious from these figures that the maximum radial and circumferential stresses belong to full ceramic and their minimum values belong to full metal disk, and for FG disks these values are located between these two extremes.

Noting that for FG and homogenous disks, the maximum values of circumferential stresses are located at the inner surface of the disk.

Distribution of non-dimensional perturbation of magnetic field vector versus dimensionless radius for different thickness profiles are shown in Figs. 11 and 12. It is seen form figures that the magnitude of perturbation of magnetic field vector decreases with increasing the grading index n. The perturbation of magnetic field vector smoothly decreases from its maximum value at the inner surface to its minimum value at the outer surface of the disk for all grading indexes.

7.1.2 Fixed-free boundary condition

The results presented in this section are according to the fixed-free boundary conditions Eq. (9). Obviously the non-dimensional temperature distribution is the same as free-free boundary condition case (Fig. 4).

The non-dimensional radial displacement versus dimensionless radius for different thickness profiles is illustrated in Figs. 13 and 14. It shows that increasing grading index n from full ceramic to full metal decreases the radial displacement. Clearly the boundary condition of displacement at the fixed inner surface is satisfied in Figs. 13 and 14. Maximum displacements occur at the outer surfaces of the disks for all grading indexes from ceramic to metal.

Figs. 15, 16, 17 and 18 show the distribution of non-dimensional radial and circumferential stresses, respectively for different thickness profiles. In both cases the maximum values belong to ceramic and the minimum values belong to metal. For FG disks, based on their grading index, their stress distribution are located between metal and ceramic extremes. As Figs. 15 and 16 show that the radial stresses are maximum

at the inner surface of the disks for all grading indexes because of the fixed boundary condition at the inner surface of the disks, however their minimum zero values at the outer surfaces satisfy the free boundary condition at the outer surfaces.

7.2 Effects of magnetic field on thermo-mechanical stresses and deformation behavior of FG rotating disks

In order to investigate the effect of uniform magnetic field

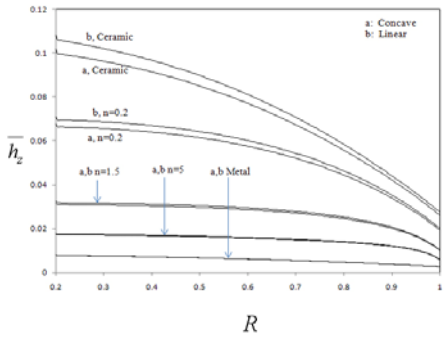

Fig. 11. Distribution of non-dimensional perturbation of magnetic field vector for concave and linear thickness profiles.

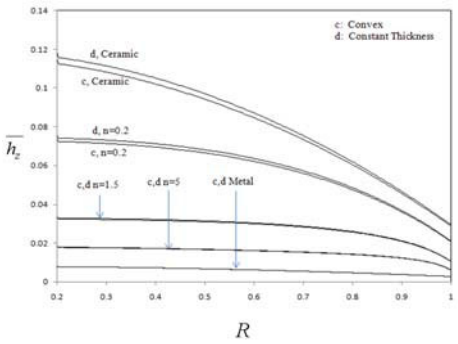

Fig. 12. Distribution of non-dimensional perturbation of magnetic field vector for convex and constant thickness profiles.

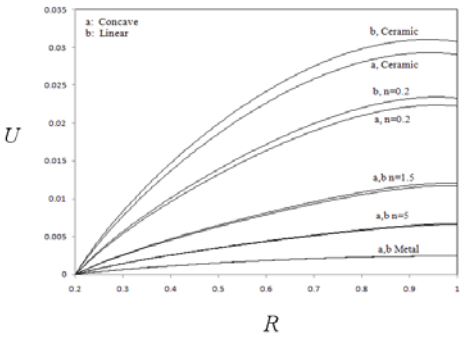

Fig. 13. Distribution of non-dimensional radial displacement for concave and linear thickness profiles.

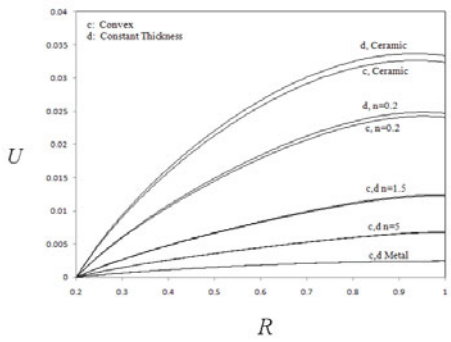

Fig. 14. Distribution of non-dimensional radial displacement for convex and constant thickness profiles.

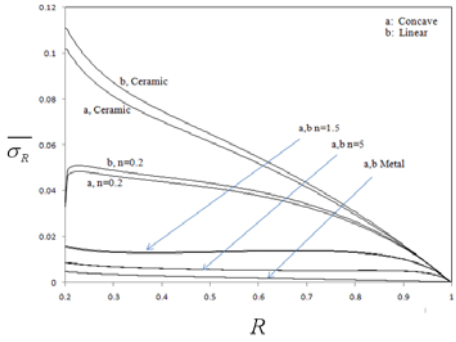

Fig. 15. Distribution of non-dimensional radial stress for concave and linear thickness profiles.

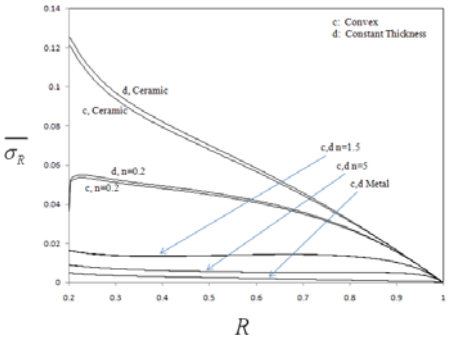

Fig. 16. Distribution of non-dimensional radial stress for convex and constant thickness profiles.

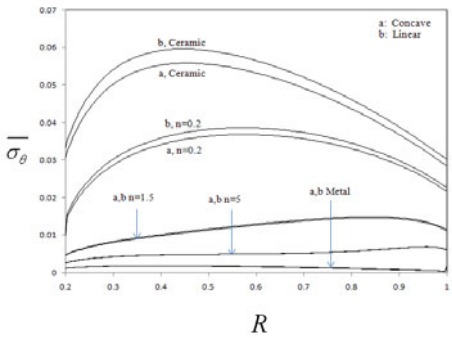

Fig. 17. Distribution of non-dimensional circumferential stress for concave and linear thickness profiles.

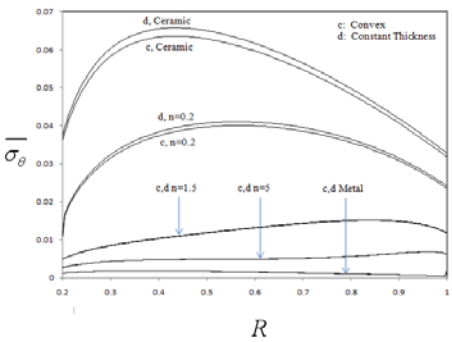

Fig. 18. Distribution of non-dimensional circumferential stress for convex and constant thickness profiles.

on mechanical behavior of the disk with concave thickness profile, the semi-analytical solution has also been carried out in the absence of magnetic field in order to compare these two cases.

7.2.1 Free-free boundary condition

Based on Sec. 5, the thermal analysis is independent of magnetic field and the magnetic field has no effect on thermal analysis. Thus the distribution of non-dimensional temperature difference along the radius is the same as shown in Fig. 4.

Fig. 19 illustrates non-dimensional radial displacement variation throughout dimensionless radii of the FG rotating disk with concave thickness profile, with and without considering the magnetic field. It shows that applying the uniform magnetic field reduces radial displacement.

Distributions of non-dimensional radial and circumferential stresses are shown in Figs. 20 and 21, respectively. It can be seen in both graphs that magnetic field significantly reduces the value of stresses.

Figs. 19, 20 and 21 show that the order of grading index from metal to ceramic has been kept the same whether or not being exposed to magnetic field.

7.2.2 Fixed-free boundary condition

The variation of non-dimensional radial displacement, radial and circumferential stresses, throughout the radius are illustrated in Figs. 22, 23 and 24, respectively. The boundary condition of zero displacement at the inner fixed condition is satisfied in Fig. 22 and the boundary condition of zero radial stress at the outer free surface of the disk is also satisfied in Fig. 23. It is obvious from Figs. 22, 23 and 24 that for this case, the discussion of previous section (section 7-1-2) is valid.

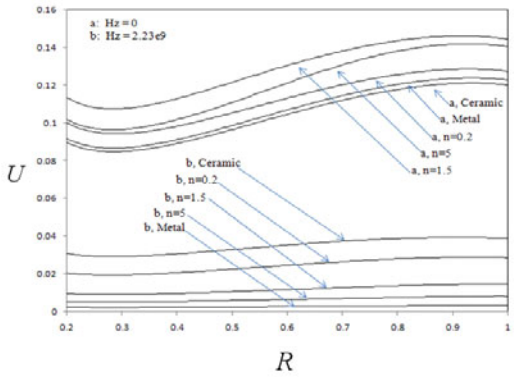

Fig. 19. Comparison of non-dimensional radial displacement with and without considering magnetic field for free-free boundary condition.

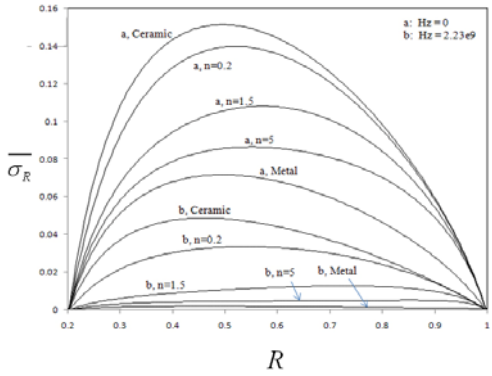

Fig. 20. Compression of non-dimensional radial stress with and without considering magnetic field for free-free boundary condition.

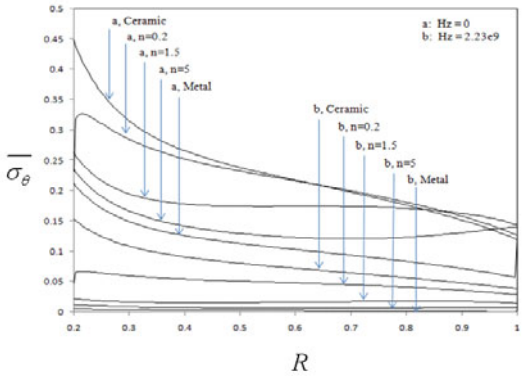

Fig. 21. Compression of non-dimensional circumferential stress with and without considering magnetic field for free-free boundary condition.

8. Conclusions

A semi-analytical solution for magneto-thermo-elasticity problem and steady state conduction heat transfer of a thin axisymmetric FG rotating disk with variable thickness has been presented. The material properties of FG disk except Poisson's ratio were modeled as the power-law distribution of volume fraction. The effects of material's grading index on the stresses, the radial displacement, the temperature, and the perturbation of magnetic field vector of the FG rotating disk have been investigated.

The following conclusions have been obtained from the present study.

(1) Except for temperature distribution which was the same for metal and ceramic, distribution of stresses, displacements and perturbation of magnetic field vectors were located between these two extremes of metal and ceramic for different values of grading index.

(2) For each disks profiles, the radial stress in FG disks decrease with increase in the value of grading index n .

(3) Except for displacement, applying magnetic field didn't change the location order of grading index.

(4) From the semi-analytical results for FG disks given in this study, it can be suggested that the gradation of the metal–ceramic components and the geometry of the disk are significant parameters in the magneto-thermo-mechanical behaviors of rotating FG disks.

(5) It is found that a FG rotating disk with parabolic thickness profile has smaller stresses and displacements compared with that of uniform thickness. Therefore, a FG rotating disk with parabolic thickness profile can be more efficient

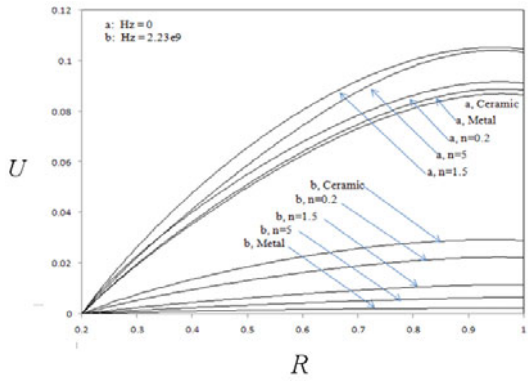

Fig. 22. Compression of non-dimensional radial displacement with and without considering magnetic field for fixed-free boundary condition.

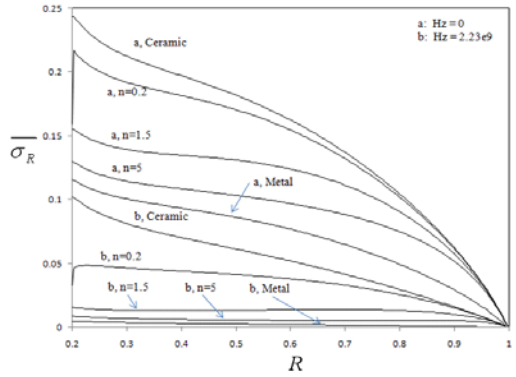

Fig. 23. Compression of non-dimensional radial stress with and without considering magnetic field fixed-free boundary condition.

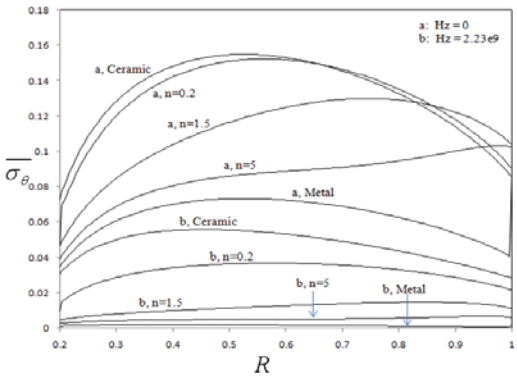

Fig. 24. Compression of non-dimensional circumferential stress with and without considering magnetic field fixed-free boundary condition.

than the one with uniform thickness.

(6) The results of stresses and displacements for concave thickness profile with and without considering the magnetic field for two different boundary conditions were compared. It has been found that a uniform magnetic field significantly decreases the tensile circumferential and radial stresses as well as the radial displacement. As a result, the fatigue life of such components can be significantly improved by imposing a magnetic field.

Acknowledgment

The authors would like to thank the referees for their valuable comments.

References

[1] S. Suresh and A. Mortensen A., Fundamentals of functionally graded materials London, K: IOM Communications Limited (1998).

[2] M. P. Lutz and R. W. Zimmerman, Thermal stresses and effective thermal expansion coefficient of a functionally graded sphere, *J. Therm. Stress*, 19 (1996) 39-54.

[3] R. W. Zimmerman and M. P. Lutz, Thermal stresses and effective thermal expansion in a uniformly heated functionally graded cylinder, *J. Therm. Stress*, 22 (1999) 177-188.

[4] SAH. Kordkheili, R. Naghdabadi, Thermoelastic analysis of a functionally graded rotating disk, *Compos Struct*., 79 (2007) 508-16.

[5] Y. Obata and N. Noda, Steady thermal stresses in a hollow circular cylinder and a hollow sphere of a functionally gradient material, *Thermal Stresses*, 17 (1994) 471-88.

[6] H. L. Dai and Y. M. Fu, Magnetothermoelastic interaction in hollow structures of functionally graded material subjected to mechanical loads, *Int. J. Press. Vessel. Pip*. 84 (2007) 132-138.

[7] H. L. Dai, Y. M. Fu and Z. M. Dong, Exact solution for functionally graded pressure vessels in a uniform magnetic field, *Int. J. Solids Struct*., 43 (2006) 5570-5580.

[8] A. Ghorbanpour, M. Salari, H. Khademizadeh and A. Arefmanesh, Magnetothermo-elastic transient response of a functionally graded thick hollow sphere subjected to magnetic and thermoelastic fields, *J. Arch. Appl. Mech*., 79 (2008) 481-497.

[9] A. Ghorbanpour, M. Salari, H. Khademizadeh and A. Arefmanesh, Magnetothermo-elastic stress and perturbation of magnetic field vector in a functionally graded hollow sphere, *J. Arch. Appl. Mech*., 80 (2010) 189-200.

[10] S. Tang, Elastic stresses in rotating anisotropic disks, International Journal of Mechanical Sciences, 11 (1968) 509-17.

[11] M. Ruhi, A. Angoshtari and R. Naghdabadi, Thermoelastic analysis of thick-walled finite-length cylinders of functionally graded materials, *Journal of Thermal Stresses*, 28 (2005) 391-408.

[12] TY. Reddy and H. Srinath, Elastic stresses in a rotating anisotropic annular disk of variable thickness and variable density, *International Journal of Mechanical Sciences*, 16 (1974) 85-9.

[13] AN. Eraslan, Elastic-plastic deformation of rotating variable thickness annular disks with free, pressurized and radially constrained boundary conditions, *International Journal of Mechanical Sciences*, 45 (2003) 643-67.

[14] U. Guven, Elastic-plastic stresses in a rotating annular disk of variable thickness and variable density, *International Journal of Mechanical Sciences*, 34 (2) (1992) 133-8.

[15] J. D. Kraus, Electromagnetic. McGraw-Hill, New York (1984).

Ali Ghorbanpour Arani received his B.Sc. degree from Sharif University of Technology in Tehran, Iran, in 1988. He then received his M.Sc. degree from Amirkabir University of Technology in Tehran, Iran, in 1991 and his Ph.D degree from the Esfahan University of Technology in Esfahan, Iran, in 2001. Dr. Ali Ghorbanpour Arani is currently a Professor at the Mechanical Engineering Department of University of Kashan in Kashan, Iran. His current research interests are stress analyses, stability and vibration of nanotubes, and FGMs.

Abbas Loghman received his B.Sc. degree from Sharif University of Technology, Tehran, Iran in 1980. He then received his MS degree from the Amirkabir University of Technology, Tehran, Iran in 1986 and his Ph.D degree from the University of Adelaide, South Australia in 1995. Dr. Loghman is an Associate Professor in the Mechanical Engineering Department of Kashan University, Kashan, Iran. His current research interests are creep and creep-fatigue life assessment of pressure vessels.

Ali Reza Shajari received his B.Sc. degree from the University of Kashan in Kashan, Iran, in 2008. He is currently a M.Sc. student at University of Kashan in Kashan, Iran. His research interests are stability and stress wave propagation in carbon nanotubes and functionally graded materials (FGMs).

Saeed Amir received his B.Sc. degree from the University of Kashan in Kashan, Iran, in 2007. He then received his M.Sc. degree from University of Kashan in Kashan, Iran, in 2009. He is currently a Ph.D student at University of Kashan in Kashan, Iran. His research interests are buckling and vibration analyses of carbon nanotubes and functionally graded materials (FGMs).